# Thermodynamic Efficiency Limits for Optically Boosted Planar Solar Cells

Y. Feng,* S. Shrestha, S. Huang, and G. Conibeer
*School of Photovoltaic and Renewable Energy Engineering, UNSW Australia, Sydney, New South Wales 2052, Australia*
(Received 2 July 2014; published 17 October 2014)

Recent attempts have been made to convert the broadband solar spectrum into filtered light, for the purpose of boosting the efficiency of a planar solar cell. By developing a thermodynamic model, the rigorous efficiency limits of the optically boosted solar cells are presented, which are achievable in principle with a piecewise function of the front emissivity or the energy-redistribution lifetime.

DOI: 10.1103/PhysRevApplied.2.044010

Efficiencies of single-junction solar cells are restricted by the Shockley-Queisser (SQ) limit [1], mainly originating from the sub-band-gap nonabsorption loss and the above-band-gap thermalization loss [2]. Approaches that attempt to bypass this limitation, including intermediate-band cells [3], hot-carrier solar cells (HCSC) [4], and multijunction cells [5] are based on the development of more advanced photovoltaic devices. On the other hand, spectral modification of the incident sunlight, including up-conversion [6] and down-conversion [7], can provide efficiency improvement on an existing single-junction solar cell.

In fact, one can view the up- and down-conversion approaches as the optical analogs of the intermediate-band cell and the multiple-exciton-generation (MEG) cell [8], respectively. A three-level up-converted solar cell can increase the photocurrent by absorbing photons with energies close to half of its band gap. Similarly, a three-level down-converted solar cell increases the photocurrent by splitting photons with energies twice its band gap into two. Just like their electrical analogs (e.g., the MEG cell), if we continuously increase the incident photon energy, these approaches have discontinuous (e.g., steppinglike) spectral responses (quantum efficiencies). This indicates that while they both provide potential improvement over single-junction solar cells, a large fraction of losses is still unavoidable even in principle.

To bypass the losses incurred in standard up- and down-conversion, recent attempts have been made on a lossless conversion from the broadband solar spectrum to near-monochromatic radiation. Such radiation spectrally matches the band-gap energy of a single-junction cell, thus ideally reducing both losses (i.e., sub-band-gap and above-band-gap losses) to zero. This approach was represented by closely related concepts, either the thermophotovoltaic converter [9–11] with filter [12] or the optical analog of HCSC [13]. Unlike up- and down-conversion, an optical bandpass filter (e.g., distributed Bragg reflector) is required to narrow down the energy exchange between the converter and the underlying photovoltaic cell within a near-monochromatic spectral region. This filter corresponds to the electrical energy-selective contacts employed in HCSCs, which is essential in order to minimize entropy generation during the extraction of carriers [14].

While the narrow bandpass filter placed between the converter and the photovoltaic cell (Fig. 1) is required in order to reduce the entropy generation associated with their energy exchange, it also imposes a restriction on the number of far-field optical modes that are available to carry the photon flux. Unless the converter and the cell is optically coupled in the near-field regime (air gap $\lesssim$ wavelength) [15], the emitter side has to have a larger surface area than the absorber side [2] in order to achieve a reasonably large number of optical modes towards the photovoltaic cell. Both options are not desirable, as near-field coupling requires an integrated design, while asymmetric surface areas do not match the planar geometry of conventional solar cells [12]. The question has been raised concerning the efficiency limit of a planar solar cell boosted by a lossless optical converter in the far-field regime.

In this work, a thermodynamic approach has been proposed, resulting in rigorous efficiency limits of optically boosted planar solar cells. The previous work on the optically coupled photovoltaic system [6,7,12,13] always assumes photon fluxes in both thermal and chemical

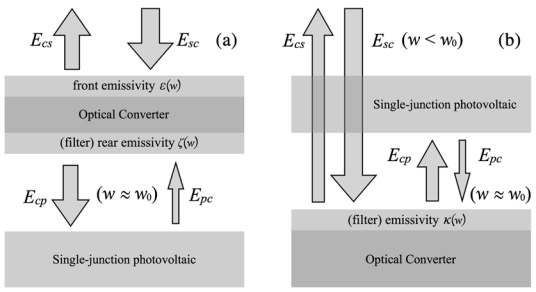


FIG. 1. Schematic diagram of the far-field coupled converter in the front configuration (a) and the back configuration (b). The bandpass filter modifies the respective emissivity function, $\zeta(w)$ or $\kappa(w)$, to a narrow rectangular window.

*yu.feng@unsw.edu.au

 

equilibrium. In addition, there is a lack of consideration on the thermodynamic details of the actual conversion process. In contrast, the model proposed in this work has fixed these deficits by adopting nonequilibrium photon statistics and taking into account the energy and entropy flows during the optical conversion. As a result, the efficiency limits provided in this work are completely rigorous, and are accessible at least in principle.

Two geometrical configurations are presented in Fig. 1 [13] which place the lossless converter at the front and at the back of the cell, respectively. Following the assumption adopted in the well-known SQ model [1], the single-junction solar cell is regarded as a blackbody (for energies above the band gap $w_0$). In the front configuration [Fig. 1(a)], the condition of energy conservation leads to

$$\int_0^\infty \varepsilon(w)E_{sc}(w)dw + \int_{w_0}^\infty \zeta(w)E_{pc}(w)dw = \int_0^\infty \varepsilon(w)E_{cs}(w)dw + \int_0^\infty \zeta(w)E_{cp}(w)dw, \quad (1)$$

equation where $\varepsilon(w)$ and $\zeta(w)$ denote the front and rear emissivities (between 0 and 1) of the converter, as functions of the photon energy $w$. In practice, they can be modified with photonic crystals. $E_{sc}$ and $E_{pc}$ represent the respective energy fluxes from the Sun and from the photovoltaic cell towards the converter, while $E_{cs}$ and $E_{cp}$ are the reverse fluxes. If assigning

$$\varepsilon(w) = \begin{cases} \kappa(w) & w \le w_0 \\ 0 & w > w_0 \end{cases}$$
$$\zeta(w) = \begin{cases} 0 & w \le w_0 \\ \kappa(w) & w > w_0 \end{cases}, \quad (2)$$

then Eq. (1) includes the back configuration as its special case, where $\kappa(w)$ is the emissivity of the converter in the back configuration [Fig. 1(b)]. Therefore, unless otherwise stated, only the front configuration will be discussed in the following content.

Spatial nonuniformity (e.g., temperature gradient) in the optical converter occurs only if different parts of the converter have limited interactions. In the extreme case, conductive and convective heat exchange do not exist; thus, different parts function as independent converters. The spatially distributed parameters, e.g., local temperature and local contributions to emissivities, optimized with respect to maximum efficiencies, must have the same values which, on the other hand, eliminate any spatial nonuniformity. Therefore, we conclude that the limiting efficiency figures can be obtained by considering spatially uniform converters only.

To convert the broadband solar spectrum into narrow-band light, the rear emissivity of the converter is nonzero only within a narrow-emission energy window (filtering), from $w_0 - \Delta/2$ to $w_0 + \Delta/2$ (Fig. 2). For photons within this range, the condition of energy conservation gives

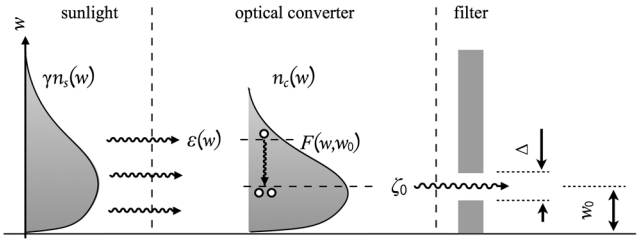


FIG. 2. Schematic of thermodynamic model and notation.

$$[(\varepsilon_0 + \zeta_0)n_0 - \gamma\varepsilon_0 n_s(w_0)]\Delta = \int_0^\infty F(w, w_0)dw, \quad (3)$$

where $\varepsilon_0$ and $\zeta_0$ are the front and rear emissivities at the photon energy $w_0$, i.e., $\varepsilon_0 = \varepsilon(w_0)$ and $\zeta_0 = \zeta(w_0)$. $\Delta$ denotes the width of the energy window. It is assumed that the variations of emissivities within the emission window are negligible. Statistical occupation functions $n_c(w)$ and $n_s(w)$ are for the respective photon populations in the converter and from the Sun, while $n_0 = n_c(w_0)$ is the photonic occupation at energy $w_0$. $\gamma = C/C_m$ is the concentration ratio $C$ normalized to its maximum value $C_m$. For planar cells, $C_m = 46\,200$ [6].

In Eq. (3), $F(w, w_0) = 4c^{-1}w_0^{-1}g^{-1}(w_0)E(w, w_0)$, which denotes the spectral flux density $E(w, w_0)$ of the total amount of photon energy redistributed from the energy level $w$ to the emission energy $w_0$, normalized by the product of $w_0$, speed of light $c$, and the optical density of states $g(w_0)$. From integration over the whole energy range (except the narrow emission window), the rate of photon generation inside the window appears at the right side of Eq. (3). For energies outside the window, the condition of energy conservation leads to

$$\varepsilon(w)[\gamma n_s(w) - n_c(w)] = (w_0/w)^3 F(w, w_0), \quad (4)$$

where the factor $(w_0/w)^3$ originates from the ratio of $w_0 g(w_0)$ to $wg(w)$.

Suppose at the temperature of the converter $T_C$, photons with the energy $w_0$ have a chemical potential $\mu_0$, i.e., its occupation $n_0$ is given by the Bose-Einstein distribution function $N(w_0; \beta_C, \mu_0)$. The redistribution of photon energy from an energy level outside the emission window $w$ to the energy right at the window $w_0$ implies change on the photon number, thus incurring variation on the total free energy. Statistically, a spontaneous process implies a reduction of free energy, i.e., $\Delta G|_{T=T_0} < 0$. This relation imposes an inequality on the chemical potentials: $p\mu(w) > q\mu_0$, where $p$ and $q$ are the numbers of involved photons before and after the conversion, while $\mu(w)$ and $\mu_0$ denote the chemical potential of photons at the energy levels $w$ and $w_0$, respectively. In conjunction with the energy conservation condition $pw = qw_0$,

$$\mu(w) > \mu_0 \frac{w}{w_0}. \tag{5}$$

This requirement is equivalent to an inequality for the photon distribution function at an arbitrary energy level $w$ outside the emission window,

$$n_c(w) > [(n_0^{-1}+1)^{w/w_0}-1]^{-1}. \tag{6}$$

To account for this thermodynamic directionality, a positive-valued lifetime $\lambda(w)$ is introduced, allowing for the net energy transfer being expressed by

$$F(w,w_0) = \frac{n_c(w) - [(n_0^{-1}+1)^{w/w_0}-1]^{-1}}{\lambda(w)}. \tag{7}$$

We further examine the physical implication of Eq. (7) by substituting a thermally equilibrated photon distribution, i.e., $n_c(w) = N(w;\beta_C,\mu)$. If the chemical potential $\mu$ is positive, the spectral density of energy redistribution $F(w,w_0)$ is positive for $w < w_0$ (photon fusion) and negative for $w > w_0$ (photon multiplication). This situation is inverted with a negative $\mu$. This implies that only one type of optical conversion (either up-conversion or down-conversion) can happen if the photons in the converter are in thermal equilibrium, while the chemical potential of photons determines which type of conversion occurs.

With semiconductor converters, a change of the photon number is usually delivered by impact ionization or its reverse Auger process. A positive photon chemical potential ($\mu > 0$) corresponds to a positive splitting of the quasi-Fermi-levels (of respective carriers), which favors the Auger recombination, while $\mu < 0$ gives rise to a net rate of carrier (and hence photon) multiplication. This directionality is consistent with the thermodynamic deduction used here.

In Eq. (7), the lifetime $\lambda(w)$ characterizes the rate of energy transfer between two energy levels $w$ and $w_0$. If $\lambda(w) \to \infty$, photons at these two levels do not interact at all. The other extreme case is $\lambda(w) \to 0$, in which the conversion (from $w$ to $w_0$) happens fast enough to maintain these photons in chemical equilibrium.

Originating from the two energy balance equations, Eqs. (3) and (4), we will solve the emitted energy flux towards the photovoltaic cell and then optimize the physical parameters for a maximum conversion efficiency. The first step is to denote the rear-emitted energy flux by $X$, which is equal to the product of the rear emissivity $\zeta_0$, the photon population $n_0$, and the width of the emission window $\Delta$, i.e., $X = \zeta_0 n_0 \Delta$. Then we express the right-hand side of Eq. (3) by $Y$, which has a physical interpretation of the total energy flux that is redistributed from other energy levels into the emission window. This transforms Eq. (3) into the following form:

$$X = \frac{\gamma\varepsilon_0\zeta_0}{\varepsilon_0+\zeta_0} n_s(w_0)\Delta + \frac{\zeta_0}{\varepsilon_0+\zeta_0} Y. \tag{8}$$

To express Eq. (4) in terms of the rear-emitted energy flux $X$ and the redistributed energy flux $Y$, we first solve the photon distribution function $n_c(w)$ by substituting Eq. (7) into Eq. (4),

$$\begin{aligned} n_c(w) =& [(n_0^{-1}+1)^{w/w_0}-1]^{-1}[\varepsilon(w)\lambda(w)w^3 w_0^{-3}+1]^{-1} \\ &+ \gamma\varepsilon(w)\lambda(w)n_s(w)[\varepsilon(w)\lambda(w)+w^{-3}w_0^3]^{-1}. \end{aligned} \tag{9}$$

Then we substitute Eq. (9) into Eq. (4) and integrate the spectral flux density of redistributed energy $F(w,w_0)$ over the whole spectrum (except the narrow emission window). According to the definition of the rear-emitted flux $X$, we replace $n_0^{-1}$ by $\zeta_0\Delta/X$ and obtain

$$Y = \int_0^\infty \frac{\gamma n_s(w) - [(\zeta_0\Delta/X+1)^{w/w_0}-1]^{-1}}{\lambda(w)+\varepsilon^{-1}(w)w_0^3/w^3}\, dw. \tag{10}$$

Equations (8) and (10) imply that the rear-emitted flux $X$ and the redistributed flux $Y$ are two interrelated variables. Equation (8) provides a monotonically increasing function $X = x(Y)$, while Eq. (10) gives rise to a monotonically decreasing function $Y = y(X)$. To maximize the rear emission $X$, both functions need to be parametrized for their maximal outputs.

The maximum function value of $x(Y)$ [Eq. (8)] is reached when the rear-side emissivity $\zeta_0$ is equal to unity. In the following content, unless otherwise stated, $\zeta_0$ is fixed at one. Now consider the partial derivative of $x(Y)$ to the front-side emissivity $\varepsilon_0$ with $Y$ substituted by $x^{-1}(X)$,

$$\left.\frac{\partial x(Y)}{\partial\varepsilon_0}\right|_{Y=x^{-1}(X)} = \frac{1}{\varepsilon_0+1}[\gamma n_s(w_0)\Delta - X]. \tag{11}$$

Equation (11) shows that the optimal value of $\varepsilon_0$ depends on the relative values of the rear emission $X$ and the concentrated solar radiation (within the emission window) $\gamma n_s(w_0)\Delta$. If $X \geq \gamma n_s(w_0)\Delta$ [or $n_0 \geq \gamma n_s(w_0)$, equivalently], the derivative is nonpositive, and $x(Y)$ reaches its maximum value when $\varepsilon_0 = 0$. Physically, the front emission has to be quenched; otherwise, it causes a greater amount of loss than the extra energy gain from absorption. On the other hand, if $X < \gamma n_s(w_0)\Delta$ the optimal value of the front emissivity $\varepsilon_0$ is equal to one.

The lifetime function $\lambda(w)$ and the emissivity function $\varepsilon(w)$ are both optimized by maximizing the function of energy redistribution $y(X)$ [Eq. (10)]. If the numerator of the integrand in Eq. (10) is positive, the optimal values are $\lambda(w) \to 0$ and $\varepsilon(w) = 1$. While with a negative numerator, the maximum function value is reached when $\lambda(w) \to \infty$ or $\varepsilon(w) = 0$. Unless the normalized concentration ratio $\gamma$ reaches unity (i.e., under full concentration), the numerator is in fact a monotonically increasing function with respect

to the photon energy $w$. We assume a critical value $w_c$ exists, which equals the numerator to zero. Therefore the numerator is positive if and only if $w > w_c$.

It is noted that Eq. (4) does not explicitly include redistributed energy fluxes between two arbitrary levels $w_1$ and $w_2$, both of which are outside the emission window. Here we will prove that this exclusion does not affect the calculation of limiting efficiencies. Without loss of generality, we suppose an inequality between the energy-normalized chemical potentials of photons at the two levels: $\mu_1/w_1 > \mu_2/w_2$. Following the thermodynamic argument adopted in Eq. (5), the net energy transfer is from $w_1$ to $w_2$, i.e., $F(w_1, w_2) > 0$. Accordingly, we modify the flux of energy redistribution, from $F(w_i, w_0)$ to $F^*(w_i, w_0)$ $(i = 1, 2)$, to maintain the validity of the energy balance equations (3) and (4):

$$\begin{aligned} F^*(w_1, w_0) &= F(w_1, w_0) + F(w_1, w_2), \\ F^*(w_2, w_0) &= F(w_2, w_0) - F(w_1, w_2). \end{aligned} \tag{12}$$

According to the optimization strategy that follows Eq. (10), for each energy level $w_i$ $(i = 1, 2)$, the optimal redistribution lifetime is either zero $[\lambda(w_i) \to 0$ if $\mu_i/w_i > \mu_0/w_0]$ or infinity $[\lambda(w_i) \to \infty$ if $\mu_i/w_i < \mu_0/w_0]$. In the latter case, photons at energy $w_i$ are decoupled from the emittable photons at $w_0$, and thus in Eq. (10) the integrand at $w_i$ has no contribution to the integral. As a result, if both $\mu_1/w_1$ and $\mu_2/w_2$ are below $\mu_0/w_0$, the energy exchange between $w_1$ and $w_2$ does not affect the performance of the converter at all, and therefore can be safely excluded.

Alternatively, we have $\mu_1/w_1 > \mu_0/w_0$, given the assumption that $\mu_1/w_1 > \mu_2/w_2$. Under optimization, this condition always yields a zero lifetime for the redistribution process between $w_1$ and $w_0$, i.e., $\lambda(w_1) \to 0$. As a result, photons at $w_1$ and $w_0$ are kept in chemical equilibrium, i.e., $\mu_1/w_1 \to \mu_0/w_0$. This, on the other hand, leads to $\mu_2/w_2 < \mu_0/w_0$, allowing a reversed energy transfer from $w_0$ back to $w_2$, i.e., $F(w_2, w_0) < 0$. Because of the directionality of energy transfer between $w_1$ and $w_2$ $[F(w_1, w_2) > 0]$, Eq. (12) modifies $F(w_i, w_0)$ to $F^*(w_i, w_0)$ while it conserves the original signs. Therefore, the energy exchange between $w_1$ and $w_2$ can be implicitly included in Eq. (7) by modifying the positive-valued lifetimes $\lambda(w_1)$ and $\lambda(w_2)$ accordingly.

Now let us find the upper boundary of the optical conversion efficiency, which is defined as the ratio of the rear emitted power to the incident power. It is noted that the rear emission $X$ is always smaller than the fully concentrated solar power $n_s(w_0)\Delta$ filtered by the emission window, as otherwise Eq. (10) would result in a strictly nonpositive $Y$, which forbids other energy levels feeding energy into the emission window. Following Eq. (11), this inequality results in optimal values of the front and rear emissivities under the maximum concentration $(\gamma = 1)$: $\varepsilon_0 = \zeta_0 = 1$. This implies a symmetric radiation from the front and rear sides within the emission window, and thus the optical conversion efficiency

$$\eta_o \triangleq \frac{w_0^3 X}{\gamma \int_0^\infty w^3 n_s(w) dw} < 50\%. \tag{13}$$

To illustrate the limiting efficiencies under lower concentrations $(\gamma < 1)$, two scenarios will be discussed.

(I) Constant functions of lifetime $\lambda(w)$ and front emissivity $\varepsilon(w)$: $\lambda(w) \equiv 0$ and $\varepsilon(w) \equiv 1$.

(II) Optimal functions of lifetime and emissivity: $\lambda(w)$ and $\varepsilon(w)$ are piecewise functions (excluding function values at the emission window) with threshold at $w_c$: $\lambda(w) = \infty$ or $\varepsilon(w) = 0$ for $w < w_c$, while $\lambda(w) = 0$ and $\varepsilon(w) = 1$ for $w > w_c$.

In case I, photons with all energies are in both thermal and chemical equilibrium. The converter is capable of absorbing the whole spectrum of sunlight and converting it into near-monochromatic light immediately. In this case, the maximum optical conversion efficiency is below 50%, irrespective of the concentration ratio $\gamma$, the emission energy $w_0$, and the window width $\Delta$.

To prove this, we need to consider only the case that $X \geq \gamma n_s(w)\Delta$, in which the optimal value of the front emissivity within the emission window $\varepsilon_0$ is equal to zero according to Eq. (11). In fact, if the rear emission $X$ is smaller than the filtered sunlight $\gamma n_s(w)\Delta$, the optical conversion efficiency $\eta_o$ is always below 50%, as a result of symmetric radiation [Eq. (13)]. Now substituting $\varepsilon_0 = 0$, $\zeta_0 = 1$, $\lambda(w) \equiv 0$, and $\varepsilon(w) \equiv 1$ into Eqs. (8) and (10), Eq. (13) is transformed to a function of $X$,

$$\eta_o(X) = \left\{1 + \left[\frac{A(X)}{X}\right] w_0\right\}^{-1}, \tag{14}$$

$$A(X) \triangleq \int_0^\infty \frac{\alpha^3 d\alpha}{\Gamma^\alpha(X) - 1} > \int_0^\infty \alpha^3 \Gamma^{-\alpha}(X) d\alpha, \tag{15}$$

where $\Gamma(X) \triangleq \Delta/X + 1$. The latter integration in Eq. (15) has the explicit solution $6[\ln \Gamma(X)]^{-4}$. For $X > 0$, $6X^{-1}[\ln \Gamma(X)]^{-4}$ has a minimum value of $1.26/\Delta$; thus,

$$\eta_o(X) < (1 + 1.26 w_0/\Delta)^{-1}. \tag{16}$$

Taking into account that the emission window is sufficiently narrow, its linewidth $\Delta$ needs to be much smaller than its center energy $w_0$, resulting in an optical conversion efficiency $\eta_o < 44\%$.

We thus conclude that case I (whole-spectrum conversion) is unable to convert more than half of the total incident power into near-monochromatic light. On the other hand, case II (optimal configuration) can give rise to a significant efficiency improvement. Two possibilities are allowed, either with a piecewise emissivity function $\varepsilon(w)$ or with a piecewise lifetime function $\lambda(w)$. In the former case,

the converter does not absorb or emit any photons below the critical energy level $w_c$. In this case, sub-$w_c$ photons are kept in equilibrium with the emittable photons with energies close to $w_0$. In contrast, in the latter case the converter can absorb photons below $w_c$, while their energy cannot be redistributed to the emission energy level $w_0$. As a result, sub-$w_c$ photons accumulate in the converter, until the reemission towards the Sun balances the absorption. Thus, a nonequilibrium distribution is established between the sub-$w_c$ and above-$w_c$ photons [Fig. 3(b)].

Shown in Fig. 3(a), an ultimate upper boundary (dashed curve) of the optical conversion efficiency $\eta_o$ can be obtained in a similar way to Eq. (16), except that in case II it is a function of the concentration ratio $\gamma$. It is noted that this boundary cannot be reached even in principle, as the derivation is based on strict inequalities, Eqs. (15) and (16). Calculated by solving the rear emission $X$ from Eqs. (8) and (10), the maximum efficiencies that are achievable in principle for $\Delta = 0.001$, 0.01, and 0.1, respectively, are illustrated by the solid curves in Fig. 3(a). In all the curves, the maximum efficiencies drop quickly with the concentration ratio $\gamma$ due to an increase of the fraction of energy lost by reemitting back to the sky.

Figure 3(b) demonstrates the emission-energy dependence of the limiting efficiencies for a fixed-emission linewidth (0.01 eV). The optimal emission energy is found to be between 0.1 and 1 eV, and is blueshifted when increasing the concentration ratio. Restricted by the narrow emission window, no efficiency enhancement (over the SQ limit) can be provided to crystallized silicon solar cells ($w_0 = 1.12$ eV), while low-band-gap cells can still greatly benefit from the optical converter.

In Fig. 3(b), the threshold (dash-dotted curve) of the optical efficiency $\eta_o$, from which enhancement of the overall photovoltaic efficiency over the SQ limit is possible, is calculated based on the assumption that the radiation from the photovoltaic cell $E_{pc}$ is negligible [Fig. 1(a)]. In reality, this radiation is reabsorbed and recycled by the converter, then contributing to the energy flux $E_{cp}$, emitted towards the cell. To account for this contribution to the overall current, Eq. (8) is reformed to

$$X = \frac{\zeta_0 Y}{\varepsilon_0 + \zeta_0} + \frac{\varepsilon_0 \zeta_0 \gamma n_s(w_0) + \zeta_0^2 n(w_0; T_{\mathrm{rm}}, qV)}{\varepsilon_0 + \zeta_0}\Delta, \qquad (17)$$

where $n(w_0; T_{\mathrm{rm}}, qV)$ is the Bose distribution function of photons emitted from the photovoltaic cell, at the room temperature $T_{\mathrm{rm}}$, and with an elevated chemical potential $qV$. The $J$-$V$ characteristics of the optically boosted cell are then expressed by

$$J = w_0^{-1}[X - \zeta_0 n(w_0; T_{\mathrm{rm}}, qV)\Delta]. \qquad (18)$$

Calculated from Eqs. (17) and (18), the boosted photovoltaic efficiencies under unconcentrated sunlight are

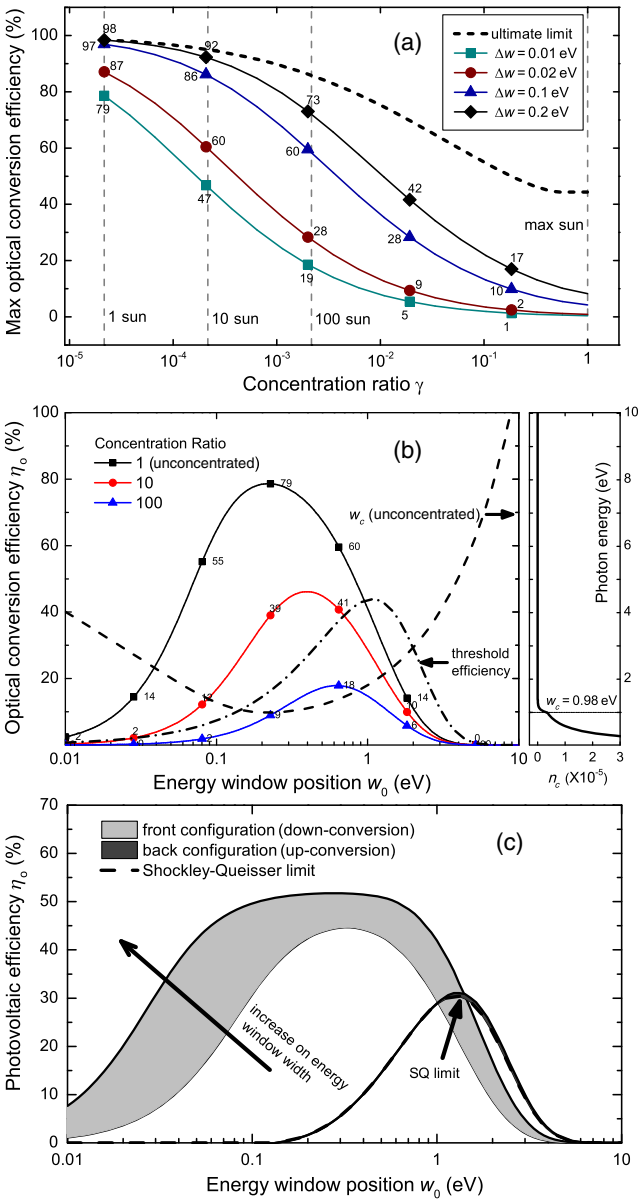


FIG. 3. (a) the ultimate limit of optical conversion efficiency as a function of the concentration level (dashed curve) and the achievable optical efficiency limits for each emission window width (solid curves). (b) Optical conversion efficiency for nondissipative converters ($\Delta = 0.01$ eV); the critical energy $w_c(w_0)$ is plotted as a dashed line for unconcentrated sunlight. The photon distribution $n_c(w)$ that gives the maximum $\eta_o$ ($w_0 = 0.22$ eV, $\eta_o = 79\%$) is plotted in the right subfigure. (c) Unconcentrated photovoltaic efficiency boosted by nondissipative optical converters. The band gap of the solar cell matches the photon energy emitted from the converter $w_0$. $\Delta$ ranges from 0.01 to 0.1 eV for both configurations. The back configuration provides only marginal enhancement over the SQ limit.

illustrated in Fig. 3(c). In the front configuration, a strong improvement over the SQ limit appears, especially for a wider window width. This is because a narrow window restricts the rear emission (optical "resistive" loss). It is noted that the

efficiency can drop if the emission window is too wide, as the entropy generation caused by radiative energy transfer between the converter and the cell relies on the window width [12]. In the back configuration [Fig. 1(b)], the marginal efficiency enhancement shown in Fig. 3(c) is calculated using a similar formulation, except that the total redistributed energy flux, Eq. (10), is integrated from 0 to $w_0$ instead.

In practice, the maximum efficiencies shown in Fig. 3 (solid curves) can be obtained by isolating sub-critical-energy (sub-$w_c$) photons from the whole conversion process. This can be accomplished by adding a high-pass filter at the front side of the converter. On the contrary, the above-critical-energy (above-$w_c$) photons should be completely absorbed and converted to emittable photons immediately. In semiconductors, this requirement is fulfilled by ultrafast elastic scattering (including intraband processes) and radiative recombination.

In conclusion, the optical converter is able to boost the planar solar cell efficiency well beyond the SQ limit. However, this cannot be achieved by a whole spectrum conversion, which is capable only of converting less than 50% of the incident power. Instead, the optimal configuration allows only for conversion of photons above a critical energy level. With an emission window width of 0.01 eV, the maximum optical conversion efficiency drops with the concentration ratio, from 79% under 1 sun down to 18% under 100 sun. With the same window width, the 1-sun photovoltaic efficiency can reach 45% with an optimal band gap of around 0.33 eV.

## ACKNOWLEDGMENTS

This program has been supported by the Australian Government through the Australian Renewable Energy Agency (ARENA). Responsibility for the views, information, or advice expressed herein is not accepted by the Australian Government. This work is also supported by NSW Government through the Science Leverage Fund.

[1] W. Shockley and H. J. Queisser, Detailed balance limit of efficiency of *p-n* junction solar cells, J. Appl. Phys. **32**, 510 (1961).

[2] M. A. Green, *Third Generation Photovoltaics: Advanced Solar Energy Conversion* (Springer, New York, 2006).

[3] A. Luque and A. Martí, Increasing the efficiency of ideal solar cells by photon induced transitions at intermediate levels, Phys. Rev. Lett. **78**, 5014 (1997).

[4] R. T. Ross and A. J. Nozik, Efficiency of hot-carrier solar energy converters, J. Appl. Phys. **53**, 3813 (1982).

[5] A. De Vos, Detailed balance limit of the efficiency of tandem solar cells, J. Phys. D **13**, 839 (1980).

[6] T. Trupke, M. Green, and P. Würfel, Improving solar cell efficiencies by up-conversion of sub-band-gap light, J. Appl. Phys. **92**, 4117 (2002).

[7] T. Trupke, M. Green, and P. Würfel, Improving solar cell efficiencies by down-conversion of high-energy photons, J. Appl. Phys. **92**, 1668 (2002).

[8] R. Brendel, J. H. Werner, and H. J. Queisser, Thermodynamic efficiency limits for semiconductor solar cells with carrier multiplication, Sol. Energy Mater. Sol. Cells **41–42**, 419 (1996).

[9] A. Lenert, D. M. Bierman, Y. Nam, W. R. Chan, I. Celanović, M. Soljačić, and E. N. Wang, A nanophotonic solar thermophotovoltaic device, Nat. Nanotechnol. **9**, 126 (2014).

[10] K. A. Arpin, M. D. Losego, A. N. Cloud, H. Ning, J. Mallek, N. P. Sergeant, L. Zhu, Z. Yu, B. Kalanyan, G. N. Parsons *et al.*, Three-dimensional self-assembled photonic crystals with high temperature stability for thermal emission modification, Nat. Commun. **4**, 2630 (2013).

[11] S. E. Han, A. Stein, and D. J. Norris, Tailoring self-assembled metallic photonic crystals for modified thermal emission, Phys. Rev. Lett. **99**, 053906 (2007).

[12] N-P. Harder and P. Würfel, Theoretical limits of thermophotovoltaic solar energy conversion, Semicond. Sci. Technol. **18**, S151 (2003).

[13] D. Farrell, Y. Takeda, K. Nishikawa, T. Nagashima, T. Motohiro, and N. Ekins-Daukes, A hot-carrier solar cell with optical energy selective contacts, Appl. Phys. Lett. **99**, 111102 (2011).

[14] Y. Feng, P. Aliberti, B. Veettil, R. Patterson, S. Shrestha, M. Green, and G. Conibeer, Non-ideal energy selective contacts and their effect on the performance of a hot carrier solar cell with an indium nitride absorber, Appl. Phys. Lett. **100**, 053502 (2012).

[15] S. Basu, Z. Zhang, and C. Fu, Review of near-field thermal radiation and its application to energy conversion, Int. J. Energy Res. **33**, 1203 (2009).